

Microtubule length distributions in the presence of protein-induced severing

Simon H. Tindemans^{1,2,*} and Bela M. Mulder^{1,†}

¹*FOM Institute AMOLF, Science Park 104, 1098 XG, Amsterdam, The Netherlands*

²*Max Planck Institute for the Physics of Complex Systems,
Nöthnitzer Strasse 38, 01187 Dresden, Germany*

(Dated: February 14, 2022)

Microtubules are highly regulated dynamic elements of the cytoskeleton of eukaryotic cells. One of the regulation mechanisms observed in living cells is the severing by the proteins katanin and spastin. We introduce a model for the dynamics of microtubules in the presence of randomly occurring severing events. Under the biologically motivated assumption that the newly created plus end undergoes a catastrophe, we investigate the steady state length distribution. We show that the presence of severing does not affect the number of microtubules, regardless of the distribution of severing events. In the special case in which the microtubules cannot recover from the depolymerizing state (no rescue events) we derive an analytical expression for the length distribution. In the general case we transform the problem into a single ODE that is solved numerically.

PACS numbers: 87.16.Ka, 87.16.ad, 87.10.Ed

I. INTRODUCTION

Microtubules are filamentous protein aggregates that appear in all eukaryotic cells. They have an inherent polarity that results in different dynamics at their two ends. The so-called plus end is highly dynamic, alternating between prolonged periods of polymerization (growth) and depolymerization (shrinkage) [1]. On the other end of the filament, the minus end often remains connected to the locus of nucleation [2] or is found to exhibit relatively steady depolymerization [3]. The combination of slow depolymerization at the minus end and prolonged growth at the plus end leads to a phenomenon known as treadmilling, whereby the individual tubulin dimers appear to move from the plus to the minus end [4]. As the stiffest of the cytoskeletal filaments, microtubules are widely used in intracellular transport and for structural support. Therefore, the dynamic properties of the microtubules are tightly regulated by the cell, often through the use of microtubule-associated proteins (MAPs) [5].

In this work we investigate one particular type of MAP that causes the severing of microtubules. It was noted by Vale [6] that otherwise stable microtubules could be severed in mitotic extracts of *Xenopus* eggs. This activity was traced back to a protein that is able to use ATP hydrolysis to sever microtubules. The protein was identified only later and given the name katanin after the katana, the Japanese Samurai sword [7]. Katanin is a heterodimer, consisting of the p60 and p80 subunits: the p80 subunit is thought to be responsible for the targeting of the protein, whereas p60 is involved in the actual severing as part of a hexameric ring [8]. The hexameric form of katanin appears to remove individual dimers from the microtubule lattice, thereby compromising the struc-

tural integrity of the microtubule. It is not currently clear whether katanin acts uniformly along the microtubule, or whether it is attracted by pre-existing lattice defects [9].

Katanin homologs have since been discovered across the animal and plant kingdoms [2]. Another severing protein by the name of spastin has also been identified. Like katanin, it also assembles in a hexameric ring, suggesting a severing mechanism similar to that of katanin [10]. Both katanin and spastin are capable of severing microtubules at seemingly random locations, and are used by the cell for the regulation of the cytoskeleton [11], for example in the mitotic and meiotic spindles [12] or the formation of the transverse cortical array in plant cells [13, 14]. Generally, the activity of severing proteins leads to a decrease in the average microtubule length, but an increase in their number [11]. Surprisingly, this increase in number can sometimes more than offset the loss of microtubule length due to the average length decrease [15].

In this work, we investigate theoretically how the occurrence of microtubule severing at random positions affects the length distribution of microtubules. Previous studies have assessed the effect of severing on actin filaments [16, 17]. However, whereas actin has a single growth mode that is described well by constant polymerization and depolymerization rates, microtubules show richer dynamics because the plus end switches between growing (polymerizing) and shrinking (depolymerizing) states.

II. MODEL

We base our model on the basic dynamic instability model that was introduced by Dogterom and Leibler [18]. In this model, microtubules exist in either the growing or the shrinking state, and switch between these states with a ‘catastrophe’ rate r_c (growth \rightarrow shrinkage) and a ‘rescue’ rate r_r (shrinkage \rightarrow growth). In the growing

*Electronic address: tindemans@amolf.nl

†Electronic address: mulder@amolf.nl

state, the microtubule extends with an effective speed v^+ , and in the shrinking state it retreats with an effective speed v^- . New microtubules are nucleated with a steady nucleation rate r_n . This set of constraints gives rise to a steady state distribution of microtubule lengths, provided that $v^+/r_c < v^-/r_r$.

We model microtubule severing by a constant severing rate per unit length. This is a valid approximation if we assume that microtubule severing process occurs on a time scale that is much shorter than the time in which a microtubule grows significantly. By taking a constant severing rate, we also implicitly assume that severing is limited by the availability of microtubules, i.e. the severing protein is available in abundance. However, because we focus on steady-state results, where the total amount of microtubules is constant, the possible invalidity of this assumption will not qualitatively affect the results.

Following the approach in [18], we construct a set of evolution equations for the length distributions of growing and shrinking microtubules. Denoting the growing and shrinking microtubule length distributions by $m^+(l, t)$ and $m^-(l, t)$, respectively, the equations can be written as

$$\frac{\partial}{\partial t} m^+(l, t) = -v^+ \frac{\partial}{\partial l} m^+(l, t) - r_c m^+(l, t) + r_r m^-(l, t) + \Phi_{severing}^+ \quad (1a)$$

$$\frac{\partial}{\partial t} m^-(l, t) = v^- \frac{\partial}{\partial l} m^-(l, t) + r_c m^+(l, t) - r_r m^-(l, t) + \Phi_{severing}^-, \quad (1b)$$

where the derivatives with respect to l reflect the translation of the distributions due to growth and shrinkage of microtubules. The severing contribution $\Phi_{severing}$ will be constructed below. These equations are supplemented by the boundary condition

$$m^+(0, t) = \frac{r_n}{v^+}, \quad (2)$$

specifying the nucleation of new microtubules with rate r_n , and by the physically motivated constraint that both distributions tend to zero for large lengths (there are no infinitely long microtubules).

In the following we derive the form of the severing terms in the set of equations (1). The inclusion of severing events leads to two types of contributions to the evolution of the length distributions: the *disappearance* flux $\phi_{out}(l, t)$ of microtubules of a certain length l and the *appearance* fluxes $\phi_{in}(l', t)$ and $\phi_{in}(l'', t)$ of two new microtubules with a total length $l = l' + l''$. In addition, the newly created microtubules can be created from microtubules that were initially growing (+) or shrinking (-). Symbolically, we write

$$\Phi_{severing}^+ = -\phi_{out}^+(l, t) + \phi_{in,+}^+(l, t) + \phi_{in,-}^+(l, t) \quad (3)$$

$$\Phi_{severing}^- = -\phi_{out}^-(l, t) + \phi_{in,+}^-(l, t) + \phi_{in,-}^-(l, t), \quad (4)$$

where $\phi_{out}^\sigma(l, t)$ stands for the removal of microtubules in state $\sigma \in \{-, +\}$, and $\phi_{in,\tau}^\sigma(l, t)$ represents the appearance of new microtubules of length l in state σ as a result

Model parameters	
v^+	growth speed
v^-	shrinkage speed
r_c	catastrophe rate
r_r	rescue rate
r_n	nucleation rate
r_s	severing rate
Dimensionless parameters	
$v = v^+/v^-$	speed ratio
$r = r_r/r_c$	rescue rate
$s = r_s v^+/r_c^2$	severing rate

Table I: Overview of the parameters in natural dimensions and the dimensionless parameters

of the severing of microtubules in state τ . The contributions will be discussed individually below.

The process of severing is controlled by the severing rate r_s that is given as a rate per unit of length. Thus we find that the fluxes of disappearing microtubules $\phi_{out}^+(l, t)$ (growing) and $\phi_{out}^-(l, t)$ (shrinking) are given by

$$\phi_{out}^+(l, t) = r_s l m^+(l, t) \quad (5)$$

$$\phi_{out}^-(l, t) = r_s l m^-(l, t). \quad (6)$$

In order to specify the influx terms $\phi_{in,\pm}^\pm$ it is necessary to specify the process of severing in more detail. We will assume that the action of the severing protein is local, thus having no effect on the remote plus and minus ends of the microtubule it severs. This implies that the plus end fragment of a severed microtubule remains in the same state. However, we must make an explicit assumption regarding the state of the newly created plus end. In line with biological observations [19], we assume that this plus end always starts out in the shrinking state. A severing event thus shortens an existing microtubule without affecting its growth state and creates an additional microtubule that is in the shrinking state. If necessary, the model can easily be extended to handle (a fraction of) severing-created plus ends that start out in the growing state.

Let us define the uniform probability density of selecting a severing location l on a microtubule of length l' as $p(l|l')$, with the value $1/l'$ for $l \in [0, l']$, and 0 otherwise. We then derive the influx $\phi_{in,+}^+(l, t)$ of growing microtubules of length l that results from the severing of growing microtubules.

$$\begin{aligned} \phi_{in,+}^+(l, t) &= \int_0^\infty \phi_{out}^+(l', t) p(l' - l|l') dl' \\ &= r_s \int_0^\infty l' m^+(l') \theta(l' - l) \frac{1}{l'} dl' \\ &= r_s \int_l^\infty m^+(l') dl', \end{aligned} \quad (7)$$

where $\theta(x)$ is the Heaviside step function. In a similar

way, and taking account the fact that the minus end fragment is always in a shrinking state, we derive

$$\begin{aligned}\phi_{\text{in},+}^{-}(l,t) &= \int_0^\infty \phi_{\text{out}}^{+}(l',t)p(l|l')dl' \\ &= r_s \int_l^\infty m^{+}(l')dl'\end{aligned}\quad (8)$$

$$\begin{aligned}\phi_{\text{in},-}^{-}(l,t) &= \int_0^\infty \phi_{\text{out}}^{-}(l',t)[p(l|l') + p(l' - l|l')]dl' \\ &= 2r_s \int_l^\infty m^{-}(l')dl'.\end{aligned}\quad (9)$$

And, because the severing of shrinking microtubules cannot produce growing microtubules, we have $\phi_{\text{in},-}^{+}(l,t) = 0$.

Note that we do not need to keep track of the correlations between the lengths of the *individual* microtubules that are created from a single cutting event, because we are looking only at ensemble-averaged length distributions. The contributions derived above are similar in form to those introduced by Edelstein-Keshet and Ermentrout [16] as the continuous limit of a discrete monomer addition and severing model for actin filaments. However, we use distinct asymmetric terms for growing and shrinking microtubules.

The model as described does not explicitly take into account the often observed depolymerization of microtubules at their minus ends that leads to treadmilling. However, this case is easily addressed through a renormalization of the growth and shrinkage speeds. Denoting the shrinkage speed at the minus end by v^{tm} , this is achieved by the substitutions $v^{+} \rightarrow v^{+} - v^{tm}$ and $v^{-} \rightarrow v^{-} + v^{tm}$, leaving the results qualitatively unchanged by the incorporation of treadmilling.

A. Steady state equations

Inserting the severing terms into equations (1) we obtain

$$\begin{aligned}\frac{\partial}{\partial t}m^{+}(l,t) &= -r_cm^{+}(l,t) + r_r m^{-}(l,t) - v^{+}\frac{\partial}{\partial l}m^{+}(l,t) \\ &\quad - r_s l m^{+}(l,t) + r_s \int_l^\infty m^{+}(l',t)dl'\end{aligned}\quad (10a)$$

$$\begin{aligned}\frac{\partial}{\partial t}m^{-}(l,t) &= +r_cm^{+}(l,t) - r_r m^{-}(l,t) + v^{-}\frac{\partial}{\partial l}m^{-}(l,t) \\ &\quad - r_s l m^{-}(l,t) + r_s \int_l^\infty [m^{+}(l') + 2m^{-}(l')]dl',\end{aligned}\quad (10b)$$

We note that in the special case when $r_c = r_r = 0$, the equation for the length distribution of the growing microtubules is equivalent to the model of microtubule GTP-cap dynamics by Flyvbjerg *et al.* [20] with a vanishing diffusion constant.

The number of parameters in these equations can be reduced by scaling the parameters and variables using

natural units for length, time and microtubule number. As a unit of time, we take the mean time to catastrophe ($1/r_c$); the unit of length is the microtubule growth in that time (v^{+}/r_c) and unit of microtubule number is the number of microtubules nucleated in this time (r_n/r_c). In terms of the dimensionless length unit $x = \frac{r_c}{v^{+}}l$, we define

$$f^{+}(x) \equiv \frac{v^{+}}{r_n}m^{+}(l(x),t) \quad (11)$$

$$f^{-}(x) \equiv \frac{v^{+}}{r_n}m^{-}(l(x),t) \quad (12)$$

$$v \equiv v^{+}/v^{-} \quad (13)$$

$$r \equiv r_r/r_c \quad (14)$$

$$s \equiv r_s v^{+}/r_c^2. \quad (15)$$

Note that the definition of v is inverted with respect to its natural conversion into dimensionless parameters, but this choice simplifies the notation in what follows. In the steady state, the equations (10) in dimensionless form become

$$\begin{aligned}\frac{d}{dx}f^{+}(x) &= -f^{+}(x) + rf^{-}(x) - sx f^{+}(x) \\ &\quad + s \int_x^\infty f^{+}(x')dx'\end{aligned}\quad (16a)$$

$$\begin{aligned}\frac{1}{v}\frac{d}{dx}f^{-}(x) &= -f^{+}(x) + rf^{-}(x) + sx f^{-}(x) \\ &\quad - s \int_x^\infty [f^{+}(x') + 2f^{-}(x')]dx',\end{aligned}\quad (16b)$$

with the boundary conditions

$$f^{+}(0) = 1 \quad ; \quad \lim_{x \rightarrow \infty} f^{+}(x) = 0 \quad ; \quad \lim_{x \rightarrow \infty} f^{-}(x) = 0. \quad (17)$$

In the absence of severing ($s = 0$) these equations are solved by the exponential functions $f^{+}(x) = e^{-(1-rv)x}$ and $f^{-}(x) = ve^{-(1-rv)x}$ [18]. Note that these solutions are only valid for $rv < 1$, when the average microtubule length is bounded.

We proceed to analyze the steady state equations (16) in a number of steps. First, we determine global properties of the length distributions. Subsequently, we derive an explicit expression for the microtubule length distributions in the special case in which rescues are absent ($r = 0$). We conclude with a numerical method using which the distribution can be calculated for arbitrary parameter values.

III. RESULTS

A. Number of microtubules

Multiplying equations (16) by x , integrating from 0 to ∞ and subtracting the results yields

$$v \int_0^\infty f^{+}(x)dx = \int_0^\infty f^{-}(x)dx. \quad (18)$$

Also, integrating over (16a) yields

$$-f^+(0) = -\int_0^\infty [f^+(x) - rf^-(x)] dx, \quad (19)$$

which can be combined with (17) and (18) to give the following expression for the total number of microtubules.

$$\int_0^\infty (f^+(x) + f^-(x)) dx = \frac{1+v}{1-rv} \quad (20)$$

Surprisingly, the total number of microtubules in the system does *not* depend on the rate of microtubule severing. Specifically, we note that severing can not prevent the diverging microtubule count for $rv \rightarrow 1$.

B. In the absence of rescue events

In the special case $r = 0$ (no rescue events), equation (16a) for $f^+(x)$ decouples from (16b) and can be solved analytically. This solution can then be used to obtain an expression for $f^-(x)$ as well. We introduce the functions $F^\pm(x) = -\int_x^\infty f^\pm(x') dx'$, allowing us to rewrite equations (16) as

$$\frac{d}{dx} \left(\frac{d}{dx} F^+(x) + (1+sx) F^+(x) \right) = 0 \quad (21)$$

$$\frac{1}{v} \frac{d^2}{dx^2} F^-(x) = -\frac{d}{dx} F^+(x) + sx \frac{d}{dx} F^-(x) + sF^+(x) + 2sF^-(x) \quad (22)$$

From equations (18) and (20) we find that $F^+(0) = -1$ (because $r = 0$), and using the boundary condition $\partial_x F^+(0) = f^+(0) = 1$ we solve (21) to obtain

$$F^+(x) = -\exp\left(-x - \frac{1}{2}sx^2\right). \quad (23)$$

Inserting this solution into equation (22), it can be solved using the boundary conditions $F^-(0) = -v$ (from equation (20)) and $\lim_{x \rightarrow \infty} F^-(0) = 0$ to give

$$F^-(x) = -v \exp\left(-x - \frac{1}{2}sv^2\right) \times \left[1 - \sqrt{\frac{\pi}{2}} \sqrt{s(1+v)} x \exp\left(\frac{(1+s(1+v)x)^2}{2s(1+v)}\right) \times \operatorname{erfc}\left(\frac{1+s(1+v)x}{\sqrt{2s(1+v)}}\right) \right], \quad (24)$$

where $\operatorname{erfc}(z)$ is the complementary error function

$$\operatorname{erfc}(y) = \frac{2}{\sqrt{\pi}} \int_y^\infty e^{-t^2} dt. \quad (25)$$

The expressions for $f^+(x)$ and $f^-(x)$ follow by differentiation of (24). The resulting distribution for $v = 1/2$ and various values of s is shown in figure 1.

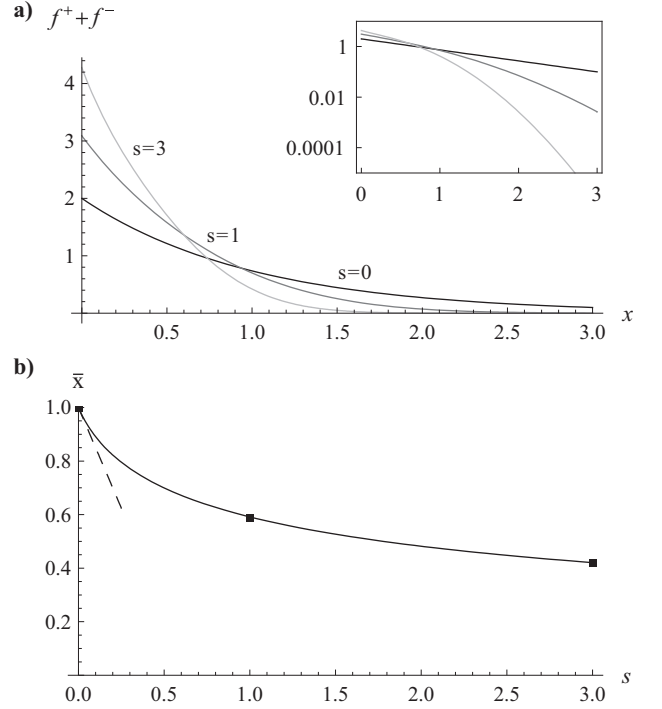


Figure 1: Results in the absence of rescues ($v = 1/2$, $r = 0$). The choice $v = 1/2$ is an approximate value based on the *in-vivo* measurements in interphase plant cells reported by Vos *et al.* [21]. **a)** Length distributions for three different values of the severing rate: $s = 0$ (black), $s = 1$ (dark gray) and $s = 3$ (light gray). The inset shows the same on a logarithmic scale. **b)** Average length as a function of the severing parameter s . The squares indicate the parameter values of the distributions in (a). The dashed line is the small- s approximation (A5). Length distributions have been calculated from (23) and (24); the average length from (29).

Looking at the derivative of the combined distribution $f^+(x) + f^-(x)$, we find that for $x = 0$

$$\frac{d}{dx} (f^+(x) + f^-(x))|_{x=0} = -(1+v)(1-s(1-2v)). \quad (26)$$

The perhaps surprising implication is that if $v < 1/2$, sufficiently high severing rates can lead to a positive slope of the distribution at $x = 0$. In other words, in that case the length distribution no longer decreases monotonically with length.

Finally, we compute the average microtubule length as

$$\bar{x} = \frac{\int_0^\infty x(f^+(x) + f^-(x)) dx}{\int_0^\infty (f^+(x) + f^-(x)) dx} \quad (27)$$

$$= -\frac{1}{1+v} \int_0^\infty (F^+(x) + F^-(x)) dx \quad (28)$$

$$= \frac{2}{z} e^{1/z^2} \int_{1/z}^\infty e^{-t^2} dt, \quad (29)$$

with $z = s(1+v)$. This confirms that the average length

decreases with increasing severing activity, a fact that is reflected in figure 1.

C. Numerical evaluation of the length distribution

For the more general case $r > 0$ we use a numerical method to solve equations (16). In order to do so, we reparameterize the problem. Inspired by the results (18) and (20) we define

$$p(x) = f^+(x) + f^-(x) \quad (30)$$

$$q(x) = v f^+(x) - f^-(x). \quad (31)$$

Hence, $p(x)$ is a (dimensionless) measure of the total microtubule density. In terms of these variables, the steady state equations (16) can be written as

$$\frac{d}{dx} q(x) = sv \left[-xp(x) + 2 \int_x^\infty p(x') dx' \right] \quad (32)$$

$$\begin{aligned} \frac{d}{dx} p(x) = & -(1-rv)p(x) - (1+r)q(x) \\ & -s(1-v)xp(x) - sq(x) + \\ & s \int_x^\infty [q(x') + (1-2v)p(x')] dx'. \end{aligned} \quad (33)$$

Equation (32) can be formally solved to give

$$q(x) = sv \int_x^\infty \left[x' p(x') - 2 \int_{x'}^\infty p(x'') dx'' \right] dx' \quad (34)$$

$$= sv \int_x^\infty [(2x-x')p(x')] dx'. \quad (35)$$

Inserting this expression into equation (33) we transform the problem into a single integral equation. We can subsequently remove the integrals by differentiating three times and obtain the linear fourth-order ODE

$$\begin{aligned} p^{(4)}(x) = & (-1+rv-s(1-v)x)p^{(3)}(x) \\ & + s(-4+v(5+x(1+r+sx)))p^{(2)}(x) \\ & + 4sv(1+r+2sx)p^{(1)}(x) + 12vs^2p(x), \end{aligned} \quad (36)$$

where $p^{(n)}(x)$ stands for $(d/dx)^n p(x)$. To derive the boundary conditions for this problem we use (20), (18) and (17) to derive

$$\int_0^\infty p(x) dx = \frac{1+v}{1-rv}, \quad (37)$$

$$\int_0^\infty q(x) dx = 0, \quad (38)$$

$$q(0) = -p(0) + 1 + v. \quad (39)$$

By repeated application of these equalities and differentiation of equations (32) and (33) we obtain the boundary

conditions

$$\begin{aligned} p^{(1)}(0) = & (1+v)rp(0) - (1+v)(1+r) \\ & + s(1+v) \left(\frac{1-2v}{1-rv} \right) \end{aligned} \quad (40)$$

$$\begin{aligned} p^{(2)}(0) = & [-r(1+v)(1-rv) + 3sv]p(0) + (1+v) \times \\ & \left[(1+r)(1-rv) - s \left(\frac{3-rv+2rv^2}{1-rv} \right) \right] \end{aligned} \quad (41)$$

$$\begin{aligned} p^{(3)}(0) = & r(1+v) [(1-rv)^2 + sr(-3+7v)]p(0) \\ & - (1+v)(1+r)(1-rv)^2 \\ & + s(1+v) [6+3r-4v-5rv+2rv^2] \\ & - s^2 \left(\frac{1+v}{1-rv} \right) (3-4v+8v^2). \end{aligned} \quad (42)$$

We note that these boundary conditions are of the form

$$\begin{pmatrix} p(0) \\ p^{(1)}(0) \\ p^{(2)}(0) \\ p^{(3)}(0) \end{pmatrix} = \mathbf{P}_1 p(0) + \mathbf{P}_2 \quad (43)$$

with a single undetermined parameter $p(0)$. Because equation (36) is a homogeneous linear ODE, we can evaluate it twice, using both \mathbf{P}_1 and \mathbf{P}_2 as boundary conditions. We generally find that both solutions diverge with opposing signs. The value of $p(0)$ can therefore be determined from the constraint $\lim_{x \rightarrow \infty} p(x) = 0$.

To this end, both solutions should be evaluated over a range that is as large as possible, whilst maintaining a very high numerical accuracy, because the final result is obtained by subtracting two diverging functions. In our numerical calculations (using Wolfram Mathematica 6.0), we have evaluated the differential equation with sufficient precision to achieve an accuracy of 13 significant digits and limited the integration range to 10 decay lengths ($x = 10(1-rv)^{-1}$) or the point at which the first solution exceeded the value 10^8 , depending on which occurred first.

Figure 2 shows the numerically computed distributions for $v = 1/2$, $r = 1$ and various values of s . It is interesting to note that the total distribution is no longer monotonically decreasing for $s = 1$ and $s = 3$. Figure 3 shows that this is solely due to the contribution from the growing microtubules. We also note that the average length decreases rapidly for relatively small severing rate. As the severing rate increases, the average length converges to that of the system without rescue events ($r = 0$). In other words, if severing events occur very frequently, rescue events are no longer significant, presumably because the microtubules become so short that they disappear before they can be rescued. This statement is summarized by the condition $1/r_r \gg \bar{l}/v^-$, where \bar{l} is the average microtubule length, or in dimensionless units $rv\bar{x} \ll 1$.

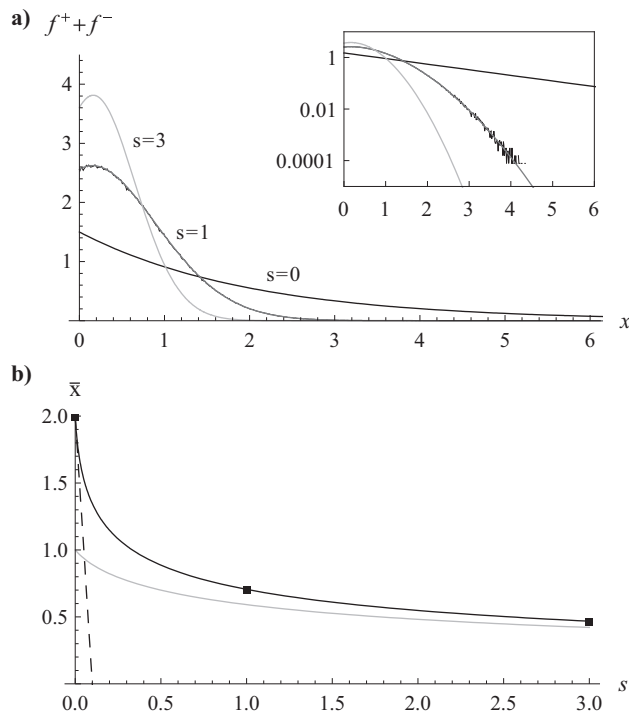


Figure 2: Numerically computed length distributions and comparison with simulation data. Based on the *in-vivo* measurements in interphase plant cells reported by Vos *et al.* [21], approximate values of $v = 1/2$ and $r = 1$ have been used. **a)** Length distributions for three different values of the severing rate: $s = 0$ (black), $s = 1$ (dark gray) and $s = 3$ (light gray). The inset shows the same on a logarithmic scale. Also shown for $s = 1$ is data obtained by a stochastic simulation of microtubule severing using a Gillespie algorithm, matching the predicted distribution. Simulation parameters were [$v^+ = 0.1 \mu\text{m s}^{-1}$, $v^- = 0.2 \mu\text{m s}^{-1}$, $r_c = 0.01 \text{s}^{-1}$, $r_r = 0.01 \text{s}^{-1}$, $r_n = 10 \text{s}^{-1}$, $r_s = 0.001 \mu\text{m}^{-1} \text{s}^{-1}$]. Length data was distributed into 500 bins and sampled 1000 times at 50 second intervals after an initial equilibration period of 50,000 seconds. **b)** Average length as a function of the severing parameter s . The squares indicate the parameter values of the distributions in (a). The dashed line is the small- s approximation (A5). The light gray curve, which converges for large s , is the result for $r = 0$ (figure 1). Length distributions have been calculated from (36).

IV. DISCUSSION

We have constructed a model that describes the dynamic instability of microtubules in combination with the severing of microtubules. This model takes the form of two coupled integro-differential equations that are a function of three parameters: v , the ratio of polymerization and depolymerization speeds, r , the ratio of the rescue and catastrophe rates, and the dimensionless severing rate s . We have analyzed the steady state solutions and their properties: notably the number of microtubules and their average length. For the special cases of no rescue

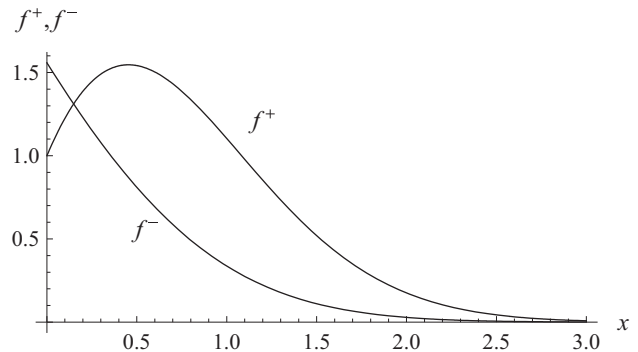


Figure 3: Length distributions for growing and shrinking microtubules separately ($v = 1/2$, $r = 1$, $s = 1$). The total distribution function $p(x) = f^+(x) + f^-(x)$ has been computed numerically using (36); $f^+(x)$ and $f^-(x)$ have been computed using (35) and (31).

events ($r = 0$) and small severing rates (see appendix A), we have presented analytical solutions. The general case has been addressed by transforming the coupled integro-differential equations into a single fourth order differential equation that is solved numerically. The resulting microtubule length distributions show a number of interesting properties.

1. Shorter, more compact length distributions

As expected, an increase in the severing rate always leads to a decrease in the average length of the microtubules. In addition, because the rate of severing is proportional to the microtubule length, the number of very long microtubules is strongly reduced, leading to a distribution that is more compact (see appendix A for an explicit expression). Furthermore, in contrast to the dynamic instability model without severing, the length distributions are no longer guaranteed to decrease monotonically with increasing length. For some parameters, a ‘bump’ is observed in the length distribution, caused by the continuous creation of short (but not vanishingly small) microtubules through the severing process.

2. Conservation of microtubule number

We have also demonstrated that the total number of microtubules does not depend on the severing rate, even though the average length of each microtubule decreases. To understand this counterintuitive result, we consider a system without severing, in which the following steady-state relation holds: [population size] = [nucleation rate] \times [average lifetime]. Suppose that a single microtubule is severed (consistent with an infinitesimally small severing rate). The expected lifetime of the created segments is obviously shorter than that of the original segment.

However, the fact that the total number of microtubules is unaffected by the presence of severing implies that this decrease in lifetime is compensated *exactly* by the fact that every severing event ‘nucleates’ an extra microtubule. For this cancellation to occur, the sum of the lifetimes of the two fragments of a severed microtubule should equal the expected lifetime of the microtubule if severing had not occurred.

That this is indeed the case can be shown using a simple argument, based on the lifetime of a microtubule in the absence of severing. In this case the dynamics of the microtubule tip are independent of its length. This implies that the average time it takes for a growing microtubule of length l to later return (in a shrinking state) to the *same* length is independent of the value of l , and therefore equal to the average microtubule lifetime T^+ (obtained by starting from $l(t_0) = 0$). The remaining contribution to the lifetime is given by the time it takes for the shrinking microtubule of length l to disappear. In the absence of rescue events, this would take a time l/v^- . However, each rescue event switches the microtubule back to the growing state, extending the microtubule’s expected lifetime by T^+ before it returns to the same position in the shrinking state. The expected number of such rescue events is equal to $r_r l/v^-$. This argument is illustrated in figure 4. Collecting the terms described above, we obtain the following expression for the expected microtubule lifetime $T(l, \sigma)$ of a microtubule of length l and growth state $\sigma \in \{-, +\}$:

$$T(l, \sigma) = T^+ \delta_{\sigma,+} + \frac{l}{v^-} (1 + r_r T^+). \quad (44)$$

The same relation, including an expression for T^+ , has been derived analytically by and Bicout [22] and an equivalent expression for microtubules that grow in discrete units was produced by Rubin [23].

Each severing event conserves the total length l of the severed microtubule and the state σ of the existing plus end, and the newly created plus end immediately undergoes a catastrophe ($\sigma_{\text{new}} = -$). In terms of life times we find that $T(l, \sigma) = T(l', \sigma) + T(l - l', -)$, so that a single severing event indeed preserves the total lifetime. By induction it follows that *any* number of severing events will leave the expected number of microtubules in the system intact.

We stress that this argument holds regardless of the frequency and location of severing events. This implies that any distribution of severing events – provided they lead to a catastrophe of the trailing end – conserves the total number of microtubules in steady state. Specifically, this also applies to severing at positions where microtubules of different orientations cross [14], a process that may be relevant to the formation of the cortical array in plant cells.

The conservation of microtubule number in the presence of severing is in apparent contradiction with the experimentally reported increase in microtubule numbers [11]. However, this can be readily explained by the fact

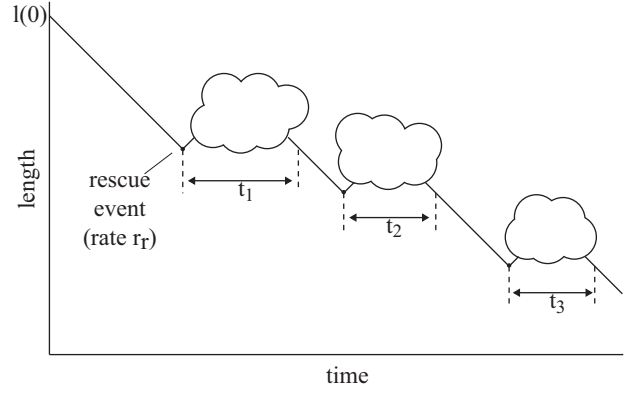


Figure 4: Schematic depiction of the life history of a shrinking microtubule with an initial length $l(0)$. The return times t_i have an expectation value T^+ .

that our results are based on the assumption of constant parameter values. In a living cell, the decrease in average microtubule length that is the result of severing will lead to an increased availability of free tubulin dimers. In turn, this is likely to increase the polymerization rate (growth speed) and nucleation rate, which would indeed cause an increase in the number of microtubules.

Acknowledgments

ST thanks Frank Jülicher and Benjamin Lindner for very helpful discussions and is grateful for the hospitality that was provided by the Max Planck Institute for the Physics of Complex Systems. The authors thank Nils Becker for critical comments on the manuscript. ST was supported by a grant from the NWO ‘‘Computational Life Sciences’’ program (contract CLS 635.100.003) and a visiting stipend from the Max Planck Society. This work is part of the research program of the ‘‘Stichting voor Fundamenteel Onderzoek der Materie (FOM)’’, which is financially supported by the ‘‘Nederlandse organisatie voor Wetenschappelijk Onderzoek (NWO)’’.

Appendix A: Small severing rates

In the absence of severing, equations (16) are solved by $f^+(x) = e^{-(1-rv)x}$ and $f^-(x) = ve^{-(1-rv)x}$. To investigate the changes that occur when a small severing rate is included, we perturb these solutions as follows

$$f^+(x) = e^{-(1-rv)x} (1 + s \hat{f}^+(x)) + O(s^2) \quad (A1)$$

$$f^-(x) = ve^{-(1-rv)x} (1 + s \hat{f}^-(x)) + O(s^2). \quad (A2)$$

Inserting these expressions into equations (16) and dropping all higher order terms gives a set of equations that

can be solved to yield

$$f^+(x) = e^{-(1-rv)x} \left(1 + s \left[\frac{1+rv^2}{(1-rv)^2} x - \frac{1+rv^2}{2(1-rv)} x^2 \right] \right) + O(s^2) \quad (\text{A3})$$

$$f^-(x) = ve^{-(1-rv)x} \left(1 + s \left[\frac{1+v}{(1-rv)^2} + \frac{-v+rv+2rv^2}{(1-rv)^2} x - \frac{1+rv^2}{2(1-rv)} x^2 \right] \right) + O(s^2) \quad (\text{A4})$$

We note that both solutions will become negative for large values of x . However, even though this is decidedly unphysical, the effect on measurable parameters such as the average microtubule length is small (for small s), because of the rapid decay of $|f^+(x)|$ and $|f^-(x)|$. The properties of the resulting distributions, such as the average length, will therefore still remain valid, subject to the bounds on s computed below.

The first-order distributions in s satisfy the total microtubule number constraint $\int_0^\infty [f^+(x) + f^-(x)] dx = (1+v)/(1-rv) + O(s^2)$, consistent with the general result (20). For the average length we obtain (to first order in s)

$$\bar{x} = \frac{1}{1-rv} - s \frac{1+v}{(1-rv)^4} + O(s^2). \quad (\text{A5})$$

For $r = 0$, this is consistent with the exact result (29). The resulting (linear) predictions are indicated in figures 1 and 2.

Finally, we determine the length variation

$$\sigma_x^2 = \langle (x - \bar{x})^2 \rangle = \frac{1}{(1-rv)^2} - k \frac{2(2+v+rv^2)}{(1-rv)^5} + O(s^2) \quad (\text{A6})$$

and, from that, the coefficient of variation (σ_x/\bar{x})

$$\sigma_x/\bar{x} = 1 - k \frac{1+rv^2}{(1-rv)^3} + O(s^2). \quad (\text{A7})$$

This number provides a measure for the relative width of the distribution. The results (A5) and (A7) confirm that severing decreases both the weighted average and the relative width of the length distribution.

The results above have been obtained under the assumption that s is very small. To make an *a priori* estimate for the validity range of s , we determine the relative importance of the terms on the right-hand side of equations (16a) and (16b). Using the results in the absence of severing as a benchmark, the terms *not* involving s give contributions of the order $(1-rv)e^{-(1-rv)x}$. Comparing the integral term (evaluated for the $s = 0$ situation) with this term gives $s \ll (1-rv)^2$. The term that is proportional to sx will dominate the other terms for large x , but this does not significantly affect the results if it only occurs for lengths that are much longer than the average length. Evaluating the terms at $x = n/(1-rv)$, where n is the number of average lengths, we obtain the constraint $s \ll (1-rv)^2/n$. Because n is of the order 1, we simply state that the approximation is accurate for $s \ll (1-rv)^2$.

-
- [1] T. Mitchison and M. Kirschner. Dynamic instability of microtubule growth. *Nature*, 312:237–242, 1984.
 - [2] D.H. Burk, R. Zhong, and Z.-H. Ye. The katanin microtubule severing protein in plants. *Journal of Integrative Plant Biology*, 49(8):1174–1182, 2007.
 - [3] S.L. Shaw, R. Kamyar, and D.W. Ehrhardt. Sustained microtubule treadmilling in Arabidopsis cortical arrays. *Science*, 300(5626):1715–1718, 2003.
 - [4] V.I. Rodionov and G.G. Borisy. Microtubule Treadmilling in Vivo. *Science*, 275(5297):215–218, 1997.
 - [5] B. Alberts, A. Johnson, J. Lewis, M. Raff, K. Roberts, and P. Walter. *Molecular Biology of the cell*. Garland Science, 4th edition, 2002.
 - [6] R.D. Vale. Severing of stable microtubules by a mitotically activated protein in xenopus egg extracts. *Cell*, 64(4):827 – 839, 1991.
 - [7] F.J. McNally and R.D. Vale. Identification of katanin, an atpase that severs and disassembles stable microtubules. *Cell*, 75(3):419 – 429, 1993.
 - [8] J.J. Hartman and R.D. Vale. Microtubule Disassembly by ATP-Dependent Oligomerization of the AAA Enzyme Katanin. *Science*, 286(5440):782–785, 1999.
 - [9] L.J. Davis, D.J. Odde, S.M. Block, and S.P. Gross. The importance of lattice defects in katanin-mediated microtubule severing in vitro. *Biophysical Journal*, 82(6):2916 – 2927, 2002.
 - [10] A. Roll-Mecak and R.D. Vale. Structural basis of microtubule severing by the hereditary spastic paraplegia protein spastin. *Nature*, 451:363–367, 2008.
 - [11] A. Roll-Mecak and R.D. Vale. Making more microtubules by severing: a common theme of noncentrosomal microtubule arrays? *J. Cell Biol.*, 175(6):849–851, 2006.
 - [12] Karen McNally, Anjon Audhya, Karen Oegema, and Francis J. McNally. Katanin controls mitotic and meiotic spindle length. *J. Cell Biol.*, 175(6):881–891, 2006.
 - [13] D.H. Burk, B. Liu, R. Zhong, W.H. Morrison, and Z.-H. Ye. A Katanin-like Protein Regulates Normal Cell Wall Biosynthesis and Cell Elongation. *Plant Cell*, 13(4):807–828, 2001.
 - [14] R. Wightman and S.R. Turner. Severing at sites of microtubule crossover contributes to microtubule alignment in cortical arrays. *Plant J.*, 52:742–751, 2007.
 - [15] M. Srayko, E.T. O’Toole, A.A. Hyman, and T. Müller-Reichert. Katanin disrupts the microtubule lattice and increases polymer number in C.elegans meiosis. *Current Biology*, 16(19):1944 – 1949, 2006.
 - [16] L. Edelstein-Keshet and G.B. Ermentrout. Models for the length distributions of actin filaments: I. Simple polymerization and fragmentation. *Bull. Math. Biol.*, 60:449–475, 1998.
 - [17] J. Roland, J. Berro, A. Michelot, L. Blanchoin, and J.-L. Martiel. Stochastic severing of actin filaments

- by actin depolymerizing factor/cofilin controls the emergence of a steady dynamical regime. *Biophysical Journal*, 94(6):2082 – 2094, 2008.
- [18] M. Dogterom and S. Leibler. Physical aspects of the growth and regulation of microtubule structures. *Phys. Rev. Lett.*, 70(9):1347–1350, 1993.
 - [19] L. Quarmby. Cellular Samurai: katanin and the severing of microtubules. *J Cell Sci*, 113(16):2821–2827, 2000.
 - [20] H. Flyvbjerg, T.E. Holy and S. Leibler. Stochastic dynamics of microtubules: a model for caps and catastrophes. *Phys. Rev. Lett.*, 73(17):2372–2375, 2004.
 - [21] J.W. Vos, M. Dogterom, and A.M.C. Emons. Microtubules become more dynamic but not shorter during preprophase band formation: a possible "search-and-capture" mechanism for microtubule translocation. *Cell Motil. Cytoskeleton*, 57(4):246–258, 2004.
 - [22] D.J. Bicout. Green's functions and first passage time distributions for dynamic instability of microtubules. *Phys. Rev. E*, 56(6):6656–6667, 1997.
 - [23] R.J. Rubin. Mean lifetime of microtubules attached to nucleating sites. *Proc. Natl. Acad. Sci. U.S.A.*, 85:446–448, 1988.